Communications

Porous and Dense Magnesium Borohydride Frameworks: Synthesis, Stability, and Reversible Absorption of Guest Species**
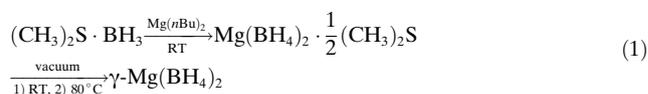
Yaroslav Filinchuk,* Bo Richter, Torben R. Jensen,* Vladimir Dmitriev, Dmitry Chernyshov, and Hans Hagemann

Hydrogen has been suggested as a carrier of renewable energy in future sustainable energy systems.[1] However, the lack of safe, compact, and efficient storage of hydrogen remains an obstacle.[2] In the solid state, hydrogen can be stored covalently bonded to a light element, for example, in complex ions BH_4^- and NH_2^-, or physisorbed in molecular form in a nanoporous material such as a metal–organic framework.[3,4] Herein we report the first light-metal hydride capable of storing molecular hydrogen. This new form of magnesium borohydride has a large permanent porosity and can also reversibly adsorb nitrogen and small molecules such as dichloromethane. We report the synthesis, stability, transformations, and structure of two new polymorphs γ- and δ-$Mg(BH_4)_2$ along with the first gas absorption experiments on porous γ-$Mg(BH_4)_2$. Our work shows that metal borohydrides and coordination polymers can have similar properties and anticipate the existence of novel hybrid materials.

Borohydride-based materials have recently received much attention owing to their high gravimetric hydrogen content and straightforward mechanochemical synthesis methods (i.e., ball milling, BM).[5,6] Drawbacks of these materials are insufficient thermodynamic and kinetic proper-

ties, and significant amounts of inert metal chlorides in the synthetic products from BM. Therefore, solution-based methods have been explored to synthesize novel metal borohydrides in a pure form.[6] Magnesium borohydride $Mg(BH_4)_2$ is one of the most promising materials for hydrogen-storage applications, as it has a relatively low decomposition temperature, reversible hydrogen desorption,[7,8] and high gravimetric hydrogen content of 14.9 wt % H_2. At present, two polymorphs of $Mg(BH_4)_2$ are known, α- and β-$Mg(BH_4)_2$; α-$Mg(BH_4)_2$ irreversibly transforms to β-Mg-$(BH_4)_2$ at $T > 490$ K.[9,10] Both polymorphs have unexpectedly complex crystal structures, which differ significantly from the numerous theoretical predictions (see Ref. [11] and references therein). Interestingly, α-$Mg(BH_4)_2$ contains 6.4 % unoccupied voids (each of 37 Å^3) in the structure.[9] These pores are too small for gas storage, but suggest the existence of more porous hydrides.

The α-phase can be obtained by removing diethyl ether or triethylamine from the corresponding solvates of Mg-$(BH_4)_2$.[6,9,12] We used a dimethylsulfide complex of borane to prepare a solvate, which, upon gentle heating, produced a new cubic polymorph, denoted γ-$Mg(BH_4)_2$, according to the reaction scheme:

[*] Prof. Y. Filinchuk
Institute of Condensed Matter and Nanosciences
Université Catholique de Louvain
place L. Pasteur 1, 1348 Louvain-la-Neuve (Belgium)
E-mail: yaroslav.filinchuk@uclouvain.be
Homepage: http://filinchuk.com/

Prof. Y. Filinchuk, B. Richter, Prof. T. R. Jensen
Center for Materials Crystallography
Interdisciplinary Nanoscience Center and
Department of Chemistry, Aarhus University
Langelandsgade 140, 8000 Aarhus C (Denmark)
E-mail: trj@chem.au.dk

Prof. Y. Filinchuk, Prof. V. Dmitriev, Dr. D. Chernyshov
Swiss-Norwegian Beam Lines at ESRF
BP-220, 38043 Grenoble (France)

Dr. H. Hagemann
Département de Chimie Physique, University of Geneva
1211 Geneva (Switzerland)

$$(CH_3)_2S \cdot BH_3 \xrightarrow[\text{RT}]{Mg(nBu)_2} Mg(BH_4)_2 \cdot \frac{1}{2}(CH_3)_2S$$
$$\xrightarrow[\text{1) RT, 2) 80°C}]{\text{vacuum}} \gamma\text{-}Mg(BH_4)_2 \qquad (1)$$

Crystal structures of the solvate and γ-$Mg(BH_4)_2$ were solved from synchrotron radiation powder X-ray diffraction (SR-PXD) data and are shown in Figure 1. Details of the synthesis, diffraction experiments, and structure solution are given in the Supporting Information.

The monoclinic solvate structure of $Mg(BH_4)_2 \cdot \frac{1}{2}S(CH_3)_2$ is a 3D framework containing two Mg atoms: one atom is tetrahedrally coordinated to four BH_4 groups, and the other to four BH_4 groups and one $S(CH_3)_2$ ligand to form a trigonal bipyramid. Removal of the $S(CH_3)_2$ ligand does not break the integrity of the framework but leads to a highly symmetric cubic structure of γ-$Mg(BH_4)_2$ (space group $Id\bar{3}a$, no. 230), where a single Mg site has a tetrahedral environment of the BH_4 groups. Its structure has a 3D net of interpenetrated channels, thus making γ-$Mg(BH_4)_2$ the first reported hydride with a large permanent porosity. The empty volume in the structure amounts to 33 %. The narrowest part of the channel is defined by a distance of 5.8 Å between hydrogen atoms, while a point at $(\frac{1}{8}, \frac{1}{8}, \frac{1}{8})$ is 3.56 Å away from the nearest H atom, 4.12 Å from the B, and 4.82 Å from the Mg atoms. The framework topology of γ-$Mg(BH_4)_2$ is isomorphous to a

11162 © 2011 Wiley-VCH Verlag GmbH & Co. KGaA, Weinheim

Angew. Chem. Int. Ed. **2011**, *50*, 11162–11166

Figure 1. Crystal structures of nanoporous Mg(BH$_4$)$_2$ and its precursor. a) Monoclinic Mg(BH$_4$)$_2$·$\frac{1}{2}$S(CH$_3$)$_2$ precursor. b) Nanoporous cubic γ-Mg(BH$_4$)$_2$. Mg atoms are shown as green spheres, BH$_4$ groups as blue tetrahedra, and unit cells are defined by red lines. The solvate contains one Mg atom in a tetrahedral environment of four BH$_4$ groups and the other in a trigonal-pyramidal environment, which also involves one S atom (yellow spheres). The structural topology of the Mg(BH$_4$)$_2$ framework is preserved upon gentle removal of the organic ligand in vacuum. Mg atoms in the resulting highly porous cubic structure are coordinated through the edges of four BH$_4$ groups.

hypothetical zeolite-type polymorph of SiO$_2$[13] and to a porous zinc imidazolate framework ZIF-72,[14] while no other materials show any similarities.

A solvent-accessible surface area of 1505 m^{2}g^{-1} was obtained from the crystal structure of γ-Mg(BH$_4$)$_2$ by using a geometrical model. This value compares well with the cumulative surface area of 1160 m^{2}g^{-1} obtained from nitrogen physisorption data by using the MP method (see the Supporting Information). Nitrogen sorption at 78 K shows very slow kinetics and low plateau pressure of 1 mbar. The pore volume distribution (see Figure S14) indicates the presence of only one type of pore of approximately 7 Å diameter, which is in good agreement with the structural model (Figure 1 b). The total pore volume is 0.60 mL g^{-1}.

The main property of the porous γ-Mg(BH$_4$)$_2$ framework is the ability to absorb guest molecules, as investigated by in situ SR-PXD. The use of the bright synchrotron source allows for the quantitative characterization of the sorption capacity and also for the localization of guest molecules, thus providing information on the host–guest interactions. We have studied the absorption of six aprotic solvents and two gases in γ-Mg(BH$_4$)$_2$ (see the Supporting Information). Among hexane, toluene, dimethylformamide, dimethylsulfoxide, chloroform, and dichloromethane, only the latter solvent is readily absorbed at room temperature and released at 313–322 K with a full recovery of the porous structure of γ-Mg(BH$_4$)$_2$. Thus, the guest insertion is reversible and uptake and release of dichloromethane is fast and complete within minutes. The framework structure remains undistorted upon absorption and shows only negligible cell expansion (linear 0.5%). Dichloromethane molecules are disordered around the threefold symmetry axis, and Rietveld refinement indicates the composition γ-Mg(BH$_4$)$_2$·0.18 CH$_2$Cl$_2$. The only relatively short host–guest contacts are the dihydrogen bonds B−H$^{δ-}$···$^{δ+}$H−C of 1.9 and 2.0 Å. There are neither substantial guest–guest interactions nor coordination of the guest to the metal atom (Mg···H−C 3.5 Å, Mg···Cl ≈ 4 Å). The host–guest interactions manifest the selectivity of the anionic borohydride groups that are capable of binding positively charged moieties.

Nitrogen and hydrogen adsorption in the rigid nanoporous γ-Mg(BH$_4$)$_2$ framework was investigated at elevated pressures and various temperatures. The comparable X-ray scattering power of H, B, N, and Mg meant that the in situ SR-PXD data enabled to localize the absorbed gas molecules unambiguously and follow their desorption in real time, at increasing temperatures, and constant pressure (see the Supporting Information for details). Figure 2 shows a significant change of the relative diffracted intensities upon nitrogen or hydrogen absorption, and Rietveld refinements revealed storage capacities of γ-Mg(BH$_4$)$_2$·0.63 N$_2$ at p(N$_2$) = 30.6 bar and γ-Mg(BH$_4$)$_2$·0.80 H$_2$ at p(H$_2$) = 105 bar; the latter

Figure 2. Gas absorption properties of the nanoporous γ-Mg(BH$_4$)$_2$. a) Low-angle section of the SR-PXD patterns for the cubic γ-Mg(BH$_4$)$_2$ under vacuum at 100 K (blue line), under 105 bar of H$_2$ at 80 K (red line), and 30.6 bar of N$_2$ at 130 K (green line). The large changes in diffracted intensities allow determination of the position and amount of physisorbed gas molecules. A disordered arrangement of gas molecules (red spheres) is shown in the inset. b) Nitrogen and hydrogen desorption isobars at p(N$_2$) = 30.6 bar and p(H$_2$) = 105 bar were determined by using Rietveld refinement on in situ synchrotron radiation powder X-ray diffraction data, λ = 0.70093 Å.

value corresponds to a total of 17.4 wt % of hydrogen stored in γ-Mg(BH$_4$)$_2$·0.80H$_2$. Similar to the adsorbed dichloromethane molecules, nitrogen or hydrogen molecules are grouped into diffuse rods centered around ($^1/_8$, $^1/_8$, $^1/_8$) and extended along the cube diagonal (x, x, x). The distances from the absorbed N and H atoms to the nearest H, B, and Mg atom of the framework are 3.07, 3.83, and more than 4 Å, respectively. These distances suggest a van der Waals interaction between gas molecules and BH$_4$ groups. The desorption isobars (see the Supporting Information) indicate that the gas molecules leave the framework at relatively high temperatures (desorption of hydrogen starts at 130 K, with ca. 50 % hydrogen remaining inside the pores at 200 K). This behavior suggests a potential for efficient hydrogen storage in related materials at moderate temperatures.

The isosteric heats of adsorption Q_{st} of nitrogen and hydrogen in γ-Mg(BH$_4$)$_2$ are determined from in situ powder diffraction data collected for 2–3 isobars at a gas pressure spanning 1.5–2 orders of magnitude (a plot of Q_{st} versus loading is shown in the Supporting Information). The Q_{st} value of approximately 15 kJ mol^{-1} for nitrogen is nearly constant with loading. An average estimate of the Q_{st} value for hydrogen is approximately 6 kJ mol^{-1} and at 15 mg H$_2$/g loading, the Q_{st} value exceeds 7 kJ mol^{-1}, which is one of the highest values among MOFs and other porous solids.[15,16]

We subsequently addressed the stability of the two polymorphs, α- and γ-Mg(BH$_4$)$_2$, which have 6.4 % and 33 % empty space, respectively, at elevated pressures. A remarkable volume collapse of approximately 20 % upon the transition from the α- to a new high-pressure polymorph of Mg(BH$_4$)$_2$ was observed at 1.1–1.6 GPa when using diamond anvil cells (DACs; see the Supporting Information). This new polymorph, denoted δ-Mg(BH$_4$)$_2$, has a tetragonal structure consisting of two interpenetrated Mg(BH$_4$)$_2$ frameworks. Each framework resembles the cristobalite structure (a polymorph of SiO$_2$), while their doubly interpenetrated arrangement has a Cu$_2$O topology, which is typical for MOFs. This structural organization is very stable, as the δ-phase is stable up to 15 GPa and upon a decompression to 1 bar, and even on heating to approximately 373 K at ambient pressure, where it transforms back to α-Mg(BH$_4$)$_2$. δ-Mg-(BH$_4$)$_2$ possesses no empty voids and has the second highest volumetric hydrogen density (147 g H$_2$/L at ambient conditions) among all known hydrides; this value is slightly below Mg$_2$FeH$_6$ with the hydrogen density of 150 g H$_2$/L. We note that the latter compound has a much lower gravimetric hydrogen density of 5.5 %, compared to 14.9 wt % in Mg-(BH$_4$)$_2$. The second highest volumetric hydrogen density in borohydrides, 127 g H$_2$/L, is recorded for the toxic Be(BH$_4$)$_2$, which has an extreme gravimetric hydrogen density of 20.7 wt %.

An even larger pressure-induced structural collapse is observed for the highly porous γ-Mg(BH$_4$)$_2$, and occurs in two steps. γ-Mg(BH$_4$)$_2$ turns into a diffraction-amorphous phase at 0.4–0.9 GPa (see Figure 3), and then at approximately 2.1 GPa into the dense δ-Mg(BH$_4$)$_2$, reaching the largest volume contraction of 44 % ever reported (either observed or predicted) for a hydride material.
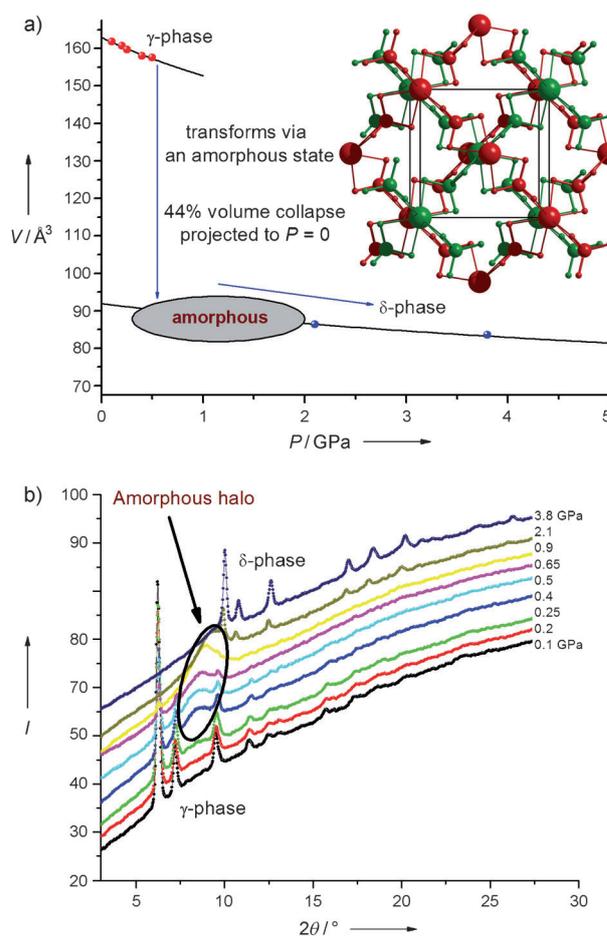
Figure 3. Pressure evolution of the nanoporous γ-Mg(BH$_4$)$_2$. a) Volume of the Mg(BH$_4$)$_2$ formula unit measured upon compression of γ-Mg(BH$_4$)$_2$ at ambient temperature. Cubic γ-Mg(BH$_4$)$_2$ transforms first into an amorphous material, which then transforms into the dense tetragonal δ-Mg(BH$_4$)$_2$. The latter contains two interpenetrated frameworks shown in green and red. The symbols represent experimental volumes and the lines are the best fits to the Murnaghan equation of state. The compressibility of δ-Mg(BH$_4$)$_2$ was studied up to 15 GPa (see the Supporting Information). b) Evolution of the SR-PXD patterns ($\lambda = 0.70040$ Å) upon compression of γ-Mg(BH$_4$)$_2$. An intermediate amorphous Mg(BH$_4$)$_2$ phase is observed in the 0.4–2.1 GPa pressure range as a broad halo with d spacing from 4.78 to 4.30 Å. At higher pressures, the amorphous material transforms to a crystalline high-pressure polymorph δ-Mg(BH$_4$)$_2$.

The specific density of the Mg(BH$_4$)$_2$ phases and their volumetric and gravimetric hydrogen contents are listed in Table 1. The experimental bulk modulus for the dense δ-Mg(BH$_4$)$_2$, 28.5(5) GPa, is much higher than for the porous polymorphs α- and γ-Mg(BH$_4$)$_2$, 10.9(4) and 12.7(12) GPa, respectively. The density of the amorphous Mg(BH$_4$)$_2$ phase obtained in the DAC cannot be determined by diffraction methods, but may be similar to δ-Mg(BH$_4$)$_2$, considering the fact that an amorphous packing of tetrahedra can be extremely dense.[17] The pressure-induced amorphization of γ-Mg(BH$_4$)$_2$ reveals another analogy to MOFs and zeolites, whose rigid porous frameworks often collapse under pressure[18,19] or upon heating to produce amorphous solids.[20] In contrast to the porous SiO$_2$,[21] an insertion of guest species,

Table 1: Specific densities (ρ) of Mg(BH$_4$)$_2$ polymorphs and their gravimetric (ρ_m) and volumetric (ρ_v) hydrogen contents ($\rho_v = \rho_m \times \rho$).

Compound	Space group	ρ [g cm^{-3}]	ρ_m [wt%]	ρ_v [g H$_2$/L]	Ref.
α-Mg(BH$_4$)$_2$	$P6_122$	0.783	14.9	117	[9]
β-Mg(BH$_4$)$_2$	$Fddd$	0.761	14.9	113	[10]
γ-Mg(BH$_4$)$_2$	$I\bar{d}3a$	0.550	14.9	82	this work
γ-Mg(BH$_4$)$_2$·0.80 H$_2$	$I\bar{d}3a$	0.565	17.4	98	this work
δ-Mg(BH$_4$)$_2$	$P4_2nm$	0.987	14.9	147	this work

for example, when nitrogen is employed as a pressure-transmitting medium, does not shift the amorphization of γ-Mg(BH$_4$)$_2$ to higher pressures. However, the most striking difference to zeolites and MOFs is the appearance of the well-crystalline δ-phase at higher pressures. Bracketing the diffraction-amorphous phase between the two crystalline polymorphs suggests some structural correlations on a short-range scale, which is indeed observed as a broad diffraction peak at 4.3–4.8 Å (see the Supporting Information). This result indicates the presence of Mg···BH$_4$···Mg fragments with corresponding characteristic Mg–Mg distances for all the crystalline phases (Table 1).

We found that ball milling of γ-Mg(BH$_4$)$_2$ produces an amorphous phase similar to that obtained by pressure-induced collapse. Detailed IR/Raman spectroscopic characterization of the amorphous and crystalline α- and β-Mg-(BH$_4$)$_2$ phases (see the Supporting Information) shows that all these phases are identical on the local level.

All the experimental polymorphs and the lowest-energy theoretical Mg(BH$_4$)$_2$ structures contain very similar local configurations: Mg atoms have a tetrahedral environment of four BH$_4$ groups, and the BH$_4$ groups are coordinated by two Mg atoms through the opposite edges. The Mg···BH$_4$ interaction is highly directional and results in linear Mg···BH$_4$···Mg fragments, which can be considered as fundamental building units in all the structures. Here the BH$_4$ group acts as a directional ligand, similar to the organic ligands ("linkers") in MOFs. On the other hand, Mg atoms form a limited set of MgH$_8$ polyhedra. Interestingly, out of all the possible eight-vertex polyhedra,[22] only the less uniform Johnson solids are found in the experimental structures, while the theoretically predicted structures always contain MgH$_8$ cubes (see the Supporting Information). The stability of MgH$_8$ coordination polyhedra can presumably be linked to the relative stability of the polymorphs. It is notable that some of the predicted Mg(BH$_4$)$_2$ structures are also highly porous or dense. These are the low-density $I\bar{4}m2$ (0.56 g cm^{-3}) and $F222$ (0.54 g cm^{-3}) structures,[23–26] which contain a single porous framework, and a dense $I4_1/amd$ (1.01 g cm^{-3}) phase that represents a doubly interpenetrated framework.[26] Although these structures are topologically similar to γ- and δ-Mg(BH$_4$)$_2$, they have not been reported to date. Both experiments and theoretical predictions suggest a vast polymorphism of Mg(BH$_4$)$_2$. Moreover, the experimentally observed phases are stable over relatively wide temperature and pressure ranges, in particular under ambient conditions, thus indicating that the reconstruction of strongly bound Mg(BH$_4$)$_2$ coordination frameworks is kinetically hindered. This behavior is likely due to

the high stability of the linear Mg···BH$_4$···Mg units, which link the MgH$_8$ nodes into various framework structures, similar to the partly covalently bonded MOFs. The relatively small charge transfer from Mg to BH$_4$ makes the bonding partly covalent and is essentially the reason for the MOF-like behavior of Mg(BH$_4$)$_2$, namely the rich polymorphism and metastability, the large pressure-induced volume collapses, and the amorphization under pressure. A possible bonding scheme involves a formation of molecular orbitals between Mg, H, and B atoms, similar to those in diborane, B$_2$H$_6$.

Porous Mg(BH$_4$)$_2$ opens up a new class of framework materials, that is, the metal borohydride frameworks, which adds to the emerging group of novel nanoporous solids, such as flexible MOFs[27] and peptides with adaptable porosity.[28] The similarity of these frameworks to MOFs provides a route to novel hybrid materials: combined use of the BH$_4^-$ ions with other directional ligands[29] may produce new porous materials, with high gas adsorption enthalpy and selectivity of absorption, demonstrated by γ-Mg(BH$_4$)$_2$. In particular, the same framework topology is observed for γ-Mg(BH$_4$)$_2$ and zinc imidazolate framework ZIF-72,[14] and thus prompts the combined use of BH$_4^-$ and imidazolate ions as ligands. On the other hand, the borohydride frameworks are significantly different from MOFs, as the former materials show specific guest–host interactions with hydridic atoms of the BH$_4^-$ ion, and have a higher structural mobility evidenced by the recrystallization of the pressure-amorphized state. It is remarkable that magnesium borohydride contains a large amount of hydrogen that can be liberated by thermolysis or hydrolysis, that is, γ-Mg(BH$_4$)$_2$ contains 14.9 wt% hydrogen bound to boron and stores an additional 3.0 wt% H$_2$ at low temperatures. Although it is difficult to practically combine the chemical and physical storage of hydrogen, γ-Mg-(BH$_4$)$_2$·0.80 H$_2$ is one of the most hydrogen-rich solids, reported to date and it is the first hydride that is capable of storing guest species. The structural data presented here are the proof-of-concept that it is possible to synthesize porous light-metal hydrides for adsorption of various gases.

Experimental Section

γ-Mg(BH$_4$)$_2$ was obtained from (CH$_3$)$_2$S·BH$_3$ and Mg(nBu)$_2$ via the Mg(BH$_4$)$_2$·½S(CH$_3$)$_2$ intermediate, evacuated at 80°C and 2×10^{-2} mbar for 12–16 h.

Crystal structures of Mg(BH$_4$)$_2$·½S(CH$_3$)$_2$, γ-Mg(BH$_4$)$_2$, γ-Mg-(BH$_4$)$_2$·0.63 N$_2$, γ-Mg(BH$_4$)$_2$·0.80 H$_2$, γ-Mg(BH$_4$)$_2$·0.18 CH$_2$Cl$_2$, and δ-Mg(BH$_4$)$_2$ were solved using synchrotron powder diffraction data measured at the Swiss–Norwegian Beam Lines of the ESRF. A monochromatic beam at calibrated wavelengths of around 0.70–0.77 Å and a MAR345 image plate detector were used. The sample-to-detector distance and parameters of the detector were calibrated using LaB$_6$ NIST standard. Details on structure solution and refinement as well as the crystallographic data are given in the supporting information.

Absorption–desorption of organic guest molecules in γ-Mg-(BH$_4$)$_2$ was monitored by wetting the sample with a solvent and following its thermodesorption by in situ SR-PXD.

Absorption–desorption of N$_2$ and H$_2$ in γ-Mg(BH$_4$)$_2$ was studied down to 80 K at pressures up to approximately 100 bar. A dosing system[30] was used to apply gas pressures on the samples enclosed in

Communications

0.5 mm glass capillaries under Ar,[31] tightly connected to the dosing system.

For high-pressure experiments, the beam was slit-collimated down to 100×100 μm^2, and α- and γ-Mg(BH$_4$)$_2$ were loaded into DACs with flat culets of 400–600 μm diameter. Ruby provided a pressure calibration with a precision of 0.1 GPa. No pressure-transmitting medium was used for α-Mg(BH$_4$)$_2$, while the γ-Mg(BH$_4$)$_2$ was compressed both in a dry form and with nitrogen as a pressure-transmitting medium. Diffraction measurements were performed up to the maximum pressure of approximately 20 GPa. Decompression experiments were followed by heating the quenched δ-phase at ambient pressure. More details and results, such as equations of state, and pressure and temperature evolution are given in the Supporting Information.

Characterization of surface area and pore size was made by physisorption of nitrogen by using a Micromeritics ASAP 2020 Surface Area and Porosity Analyzer. IR/Raman spectra were collected using a Biorad Excalibur instrument/488 nm laser combined with a Kaiser Optical Holospec monochromator and liquid nitrogen cooled CCD camera.

[1] D. J. C. MacKay, *Sustainable Energy—Without Hot Air*, UIT, Cambridge, England, **2009**.

[2] U. Eberle, M. Felderhoff, F. Schüth, *Angew. Chem.* **2009**, *121*, 6732–6757; *Angew. Chem. Int. Ed.* **2009**, *48*, 6608–6630.

[3] S.-I. Orimo, Y. Nakamori, J. R. Eliseo, A. Züttel, C. M. Jensen, *Chem. Rev.* **2007**, *107*, 4111–4132.

[4] B. Panella, M. Hirscher in *Handbook of Hydrogen Storage* (Ed.: M. Hirscher), Wiley-VCH, Weinheim, **2010**, pp. 39–59.

[5] a) V. V. Volkov, K. G. Myakishev, *Inorg. Chim. Acta* **1999**, *289*, 51–57; b) D. Ravnsbæk, Y. Filinchuk, Y. Cerenius, H. J. Jakobsen, F. Besenbacher, J. Skibsted, T. R. Jensen, *Angew. Chem.* **2009**, *121*, 6787–6791; *Angew. Chem. Int. Ed.* **2009**, *48*, 6659–6663.

[6] H. Hagemann, R. Černý, *Dalton Trans.* **2010**, *39*, 6006–6012.

[7] G. Severa, E. Rönnebro, C. M. Jensen, *Chem. Commun.* **2010**, *46*, 421–423.

[8] R. J. Newhouse, V. Stavila, S.-J. Hwang, L. E. Klebanoff, J. Z. Zhang, *J. Phys. Chem. C* **2010**, *114*, 5224–5232.

[9] Y. Filinchuk, R. Černý, H. Hagemann, *Chem. Mater.* **2009**, *21*, 925–933.

[10] J.-H. Her, P. W. Stephens, Y. Gao, G. L. Soloveichik, J. Rijssenbeek, M. Andrus, J.-C. Zhao, *Acta Crystallogr. Sect. B* **2007**, *63*, 561–568.

[11] Z. Łodziana, M. J. van Setten, *Phys. Rev. B* **2010**, *81*, 024117.

[12] P. Zanella, L. Crociani, N. Masciocchi, G. Giunchi, *Inorg. Chem.* **2007**, *46*, 9039–9041.

[13] M. D. Foster, O. D. Friedrichs, R. G. Bell, F. A. A. Paz, J. Klinowski, *J. Am. Chem. Soc.* **2004**, *126*, 9769–9775.

[14] R. Banerjee, A. Phan, B. Wang, C. Knobler, H. Furukawa, M. O'Keeffe, O. M. Yaghi, *Science* **2008**, *319*, 939–943.

[15] B. Schmitz, U. Muller, N. Trukhan, M. Schubert, G. Férey, M. Hirscher, *ChemPhysChem* **2008**, *9*, 2181–2184.

[16] S. Barman, H. Furukawa, O. Blacque, K. Venkatesan, O. M. Yaghi, H. Berke, *Chem. Commun.* **2010**, *46*, 7981–7983.

[17] A. Jaoshvili, A. Esakia, M. Porrati, P. M. Chaikin, *Phys. Rev. Lett.* **2010**, *104*, 185501.

[18] K. W. Chapman, G. J. Halder, P. J. Chupas, *J. Am. Chem. Soc.* **2009**, *131*, 17546–17547.

[19] G. N. Greaves, F. Meneau, A. Sapelkin, I. Gwynn, S. Wade, G. Sankar, *Nat. Mater.* **2003**, *2*, 622–629.

[20] T. D. Bennett, D. A. Keen, J.-C. Tan, E. R. Barney, A. L. Goodwin, A. K. Cheetham, *Angew. Chem.* **2011**, *123*, 3123–3127; *Angew. Chem. Int. Ed.* **2011**, *50*, 3067–3071.

[21] J. Haines, O. Cambon, C. Levelut, M. Santoro, F. Gorelli, G. Garbarino, *J. Am. Chem. Soc.* **2010**, *132*, 8860–8861.

[22] D. Casanova, M. Llunell, P. Alemany, S. Alvarez, *Chem. Eur. J.* **2005**, *11*, 1479–1494.

[23] V. Ozolins, E. H. Majzoub, C. Wolverton, *Phys. Rev. Lett.* **2008**, *100*, 135501.

[24] X.-F. Zhou, Q.-R. Qian, J. Zhou, B. Xu, Y. Tian, H.-T. Wang, *Phys. Rev. B* **2009**, *79*, 212102.

[25] R. Caputo, A. Tekin, W. Sikora, A. Züttel, *Chem. Phys. Lett.* **2009**, *480*, 203–209.

[26] J. Voss, J. S. Hummelshøj, Z. Łodziana, T. Vegge, *J. Phys. Condens. Matter* **2009**, *21*, 012203.

[27] C. Serre, C. Mellot-Draznieks, S. Surblé, N. Audebrand, Y. Filinchuk, G. Férey, *Science* **2007**, *315*, 1828–1831.

[28] J. Rabone, Y.-F. Yue, S. Y. Chong, K. C. Stylianou, J. Bacsa, D. Bradshaw, G. R. Darling, N. G. Berry, Y. Z. Khimyak, A. Y. Ganin, P. Wiper, J. B. Claridge, M. J. Rosseinsky, *Science* **2010**, *329*, 1053–1057.

[29] M. J. Ingleson, J. P. Barrio, J. Bacsa, A. Steiner, G. R. Darling, J. T. A. Jones, Y. Z. Khimyak, M. J. Rosseinsky, *Angew. Chem.* **2009**, *121*, 2046–2050; *Angew. Chem. Int. Ed.* **2009**, *48*, 2012–2016.

[30] P. L. Llewellyn, P. Horcajada, G. Maurin, T. Devic, N. Rosenbach, S. Rosenbach, C. Serre, D. Vincent, S. Loera-Serna, Y. Filinchuk, G. Férey, *J. Am. Chem. Soc.* **2009**, *131*, 13002–13008.

[31] T. R. Jensen, T. K. Nielsen, Y. Filinchuk, J.-E. Jørgensen, Y. Cerenius, E. M. Gray, C. J. Webb, *J. Appl. Crystallogr.* **2010**, *43*, 1456–1463.